Geographic Routing in Multilevel Scenarios of Vehicular Ad Hoc Networks

Lina Zhu, Changle Li, *Member, IEEE,* Bingbing Li, Xinbing Wang, *Senior Member, IEEE,* and Guoqiang Mao, *Senior Member, IEEE*

***Abstract*—Vehicular ad hoc networks (VANETs) present a multilevel feature when vehicles move in multilevel scenarios, such as viaducts, tunnels and ramps. Different from the city and highway scenarios, the complicated node distribution and transmission condition make the routing decision more challenging in the multilevel environment. To address the issue, this paper investigates geographic routing protocols for the multilevel scenario of VANETs. We first reveal the impacts of the multilevel feature on network characteristics by an outdoor transmission experiment and a stochastic analysis. In particular, the measured data and analysis results show that the wireless transmission range dramatically degrades, which deteriorates the connectivity probability and the performance of geographic routing protocols in the network. Motivated by the above results, we propose a Multilevel scenario oriented Greedy Opportunity Routing protocol (M-GOR). In the protocol, we present a calculation method for the connectivity probability, and a greedy opportunity forwarding algorithm to respond the impacts of the multilevel structure. Both the analysis and simulation results demonstrate benefits of M-GOR in terms of the average hop count and delivery ratio.**

***Index Terms*—VANET, multilevel, routing.**

I. Introduction

Vehicular ad hoc networks (VANETs) facilitate a variety of attractive applications related to safety (e.g., collision detection and warning) and infotainment (e.g., information sharing and mobile office). The potential market value motivates the rapid development of new communication technologies [1]. Among all, the routing protocol is one of the most crucial technologies due to its responsibility for the route selection [2].

Originally, noteworthy pioneering works [3] [4] have laid the foundation that using the greedy forwarding (GF) algorithm for the routing decision in VANETs. Recently, lots of efforts are devoted to dealing with the challenges posed by special scenarios, such as the city [5] and highway scenarios [6]. Then, some notable achievements are motivated [7]. However, besides the two scenarios, the multilevel structure becomes increasingly popular due to its effectiveness on the land use. The structure contains viaducts, tunnels and ramps, which attracts not only counties with limited land resources but also countries with abundant land resources. Therefore, the high quality routing protocol is necessary for the multilevel scenario due to the popularity. However, the existence of the multilevel structure makes the node distribution more complicated, which induces new problems to routing.

Firstly, the node distribution becomes more complicated, because vehicles are on different road levels. Thus, two communication modes are induced, i.e., the intra-level and inter-level communications. The intra-level communication occurs if the transmitter and receiver are on the same level, while the inter-level communication occurs if the two nodes are on different levels. In particular, the channel quality gets worse due to more serious path loss and interference induced by the multilevel structure, which leads to a degradation of the transmission range in the inter-level communication [8] [9]. Then, the degradation potentially influences the routing performance [10]. Secondly, the connectivity probability [11] depends on the transmission range and node distribution in the network [12]. It reduces with the transmission degradation in the multilevel VANET, which then influences the routing performance. Thirdly, the relay is selected in the relay selection region (RSR) that is the available neighbor set of the transmitter (as shown in Fig. 1) [10]. However, RSR contains two kinds of nodes in the multilevel VANET, i.e., the intra-level neighbor and inter-level neighbor. The intra-level neighbor indicates the neighbor locating on the same

 This work was supported by the National Natural Science Foundation of China under Grant No. 61271176, No. 61401334 and No. 61571350, the Fundamental Research Funds for the Central Universities (BDY021403, JB140113), and the 111 Project (B08038).

L. Zhu, C. Li, and B. Li are with the State Key Laboratory of Integrated Services Networks, Xidian University, China. X. Wang is with the Department of Electronic Engineering, Shanghai Jiao Tong University, China. G. Mao is with University of Technology Sydney, Australia. (Corresponding author: Changle Li, e-mail: clli@mail.xidian.edu.cn)

level with the transmitter, while the inter-level neighbor is the neighbor locating on different levels respecting to the transmitter. The relay selection needs a balance when the inter-level neighbor has the furthest routing progress and the intra-level neighbor has better quality of channel. For instance, the inter-level neighbor of S1 (i.e., node A in Fig. 1) has the furthest routing progress, because the distance between A and S1 is longer than the distance between S1 and B, where B is an intra-level neighbor of S1. Conversely, B has good channel quality without obstacles. This makes the routing decision more difficult.

All above problems make the existing system model and mobility model inapplicable, and routing more difficult. However, the research of the routing protocol in the multilevel VANET is rarely involved [13]. To address the issue, this paper investigates routing protocols for the multilevel scenario in VANETs. We first build the system model according to the real traffic system. Based on the model, an outdoor transmission experiment is introduced and closed-form equations are derived, which reveal the impacts of the multilevel structure. In particular, we present three important results in the multilevel VANET. (1) The transmission range dramatically degrades in the inter-level communication. (2) The connectivity probability reduces compared with the value without the transmission degradation. (3) The traditional geographic routing protocol deteriorates in terms of the average hop and delivery ratio. Motivated by the above results, we propose a Multilevel scenario oriented Greedy Opportunity Routing protocol (M-GOR). In the protocol, we present a calculation method of the connectivity probability for the direction selection at the intersection, and a greedy opportunity forwarding algorithm for the relay selection on the road segment. In the end, we execute simulations on the network layer and system level. Both analysis and simulation results show benefits of M-GOR in the multilevel vehicular network. The main contributions of the paper are summarized as follows.

- By an outdoor transmission experiment and a stochastic analysis, we reveal that the existence of the multilevel scenario causes dramatic degradations in the wireless transmission range and connectivity probability, which then deteriorate the performance of geographic routing protocols.
- We propose M-GOR for routing in the multilevel VANET. In particular, a calculation method for the connectivity probability and a greedy opportunity forwarding algorithm are presented in the protocol.
- We conduct simulations from both the network layer and system level. Specifically, the proposed M-GOR and two existing protocols are simulated by the network simulator NS-2.34. Results show that M-GOR performs well in multilevel VANETs.

The remainder of the paper is organized as follows. We describe the related work and motivation in Section II. We build the system model according to the real multilevel structure in Section III. Section IV describes the impacts of the multilevel scenario on VANETs. In Section V, we propose M-GOR for the multilevel VANET, and analyze its performance. We make simulations in Section VI. In the end, we conclude the paper.

II. Related Work and Motivations

A. Related Work

Routing enables a message to pass from the source to destination, which is a key feature of wireless networks. In VANETs, different types of routing protocols are proposed to deal with challenges in vehicular environments, which are ad hoc, geographic, cluster based, broadcast and geocast routing [14]. Among all, the geographic routing protocol is one of the most attractive routing technologies for VANETs.

In the protocol, a node makes the routing decision only depending on its local location information. Utilizing the GPS device, hello scheme [15] and location service system [16], any node can obtain locations of itself, its neighbors and the destination. Without the route construction and maintenance phases, the geographic routing protocol is suitable and widely adopted in VANETs. The pioneering achievement is GPSR [3]. In this work, Karp and Kung use the GF algorithm to select the next relay. The transmitter transmits the packet to the neighbor that is geographically closest to the destination. However, the complex traffic environment contains different terrains, such as the city and highway, which pose separate challenges to routing protocols in VANETs. Intersections place a unique challenge to routing in the city vehicular network [17]. The highway environment induces a serious issue of intermittent connection [18]. Later on, new studies are developed for these special scenarios. Focusing on the serious intermittently connected problem, Wisitpongphan et al. [19] develop a linear analysis framework to discuss the network characteristics in the highway VANET. For the single-hop communication, Abboud and Zhuang [20] make analysis on the link characteristics, while Luan et al. [18] discuss the integrity-oriented content transmission. In [21], authors use the prediction algorithm to deal with the intermittent connectivity problem in multi-hop communication. In the city VANET, noteworthy works make the routing decision at the intersection and on the road segment separately to circumvent the challenge

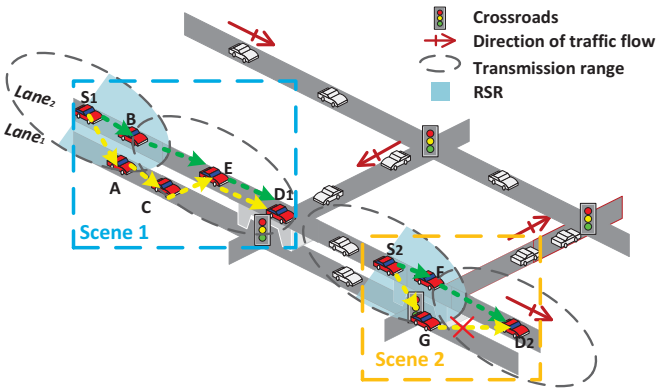

Fig. 1. Illustration of the multilevel scenario.

placed by the intersection. These works include greedy perimeter coordinator routing (GPCR) [4], connectivity-aware routing (CAR) and its improved versions[22-24], static-node-assisted adaptive data dissemination protocol (SADV) [25] and back-bone-assisted hop greedy routing (BAHG) [17]. In the type of protocols, the packet is transmitted along the road segment by GF algorithm hop by hop. The transmitter will choose the next transmission direction/segment based on the distance or the connectivity probability at the intersection. The issue of intermittent connectivity also exists in the city VANET. To address the issue, protocols, such as greedy traffic aware routing protocol (GyTAR) [26] and vehicle-assisted data delivery (VADD) [27], utilize the carry and forward algorithm, in which the transmitter will carry the packet by itself if it cannot find an available neighbor for delivery. In addition, the methods of mobility-aware [28] and multipath [29] are also introduced to address the issue.

However, almost all geographic routing protocols are designed for 2D scenarios containing the city and highway [30] [31], while the issue of routing is rarely involved in 3D scenarios, such as the multilevel VANET [32]. In 2013, Lin et al. [13] propose a three-dimensional routing protocol for the multilevel VANET. However, the protocol defines that only the intra-level neighbor of the transmitter can be selected as the next relay, although it might be an improper relay. Furthermore, both the calculation method of the connectivity probability and the intermittently connected problem are not addressed.

B. Motivation

Intuitively, a degradation of the wireless transmission range should exist due to more complicated node distribution, more serious signal fading and worse channel quality in the multilevel scenario. Based on the degradation, the connectivity first has a reduction. Therefore, geographic routing protocols suffer the influences of the poor routing decision at the intersection.

TABLE I
MAJOR NOTIONS

λ_i	Node density of traffic lane $Lane_i$.
$V_{i,j}$	The jth vehicle on $Lane_i$.
$S_{i,j}$	Spacing between node $V_{i,j-1}$ and $V_{i,j}$.
R	Transmission range of intra-level communication.
$R^{'}$	Transmission range of inter-level communication.
δ	Degradation rate of transmission range $\delta = R/R^{'}$.
X_{Near}	Spacing between the reference node and its nearest intra-level node.
Y_{Near}	Spacing between the reference node and its nearest inter-level node.
X_i	The ith one-hop progress when routing on $Lane_1$.
Y_i	The ith one-hop progress when routing on $Lane_2$.
$N_{i,[a,b]}$	The number of node in the range $[a,b]$ on $Lane_i$.
l_A	Coordinate of node A.
A_{id}	ID of node A.
$D_{A,B}$	Distance between node A and node B.
C_{ideal}	Probability without available neighbors when $\delta = 0$.
C_{real}	Probability without available neighbors when $\delta \neq 0$.
p_{Gh}/p_{Th}	The probability of hop increase caused by the inter-level delivery in GF/GOF.
p_{Gd}/p_{Td}	The probability of delivery decrease caused by the inter-level delivery in GF/GOF.

Moreover, the GF algorithm has a predominant position in routing protocols of VANETs. In the algorithm, the transmitter selects the neighbor who makes the longest progress towards the destination as the relay. However, the chosen node might be a bad relay in the multilevel VANET, if the node is an inter-level neighbor of the transmitter. Then, the bad relay induces the issues of hop count increase and delivery ratio decrease. We can give two instances as follows.

Scene 1 depicts the issue of hop increase in Fig. 1. The transmitter S_1 has two neighbors, i.e., the inter-level neighbor A and intra-level neighbor B. Depending on the GF algorithm, S_1 selects its furthest neighbor A as the relay. Then, the packet arrives at the destination D_1 along path $S_1 - A - C - E - D_1$ with 4 hops. However, node B can touch a better node E directly, because the intra-level communication has longer transmission range. The route $S_1 - B - E - D_1$ just needs 3 hops. Hence, the GF algorithm potentially causes a higher hop count due to the existence of two kinds of neighbors in the multilevel VANET.

Scene 2 indicates the issue of delivery ratio decrease. The transmitter S_2 delivers the packet to its inter-level neighbor G based on the GF algorithm. Then, G will drop the packet without available neighbors. However, the performance will be better if S_2 originally transmits the packet to its intra-level neighbor F. Therefore, the

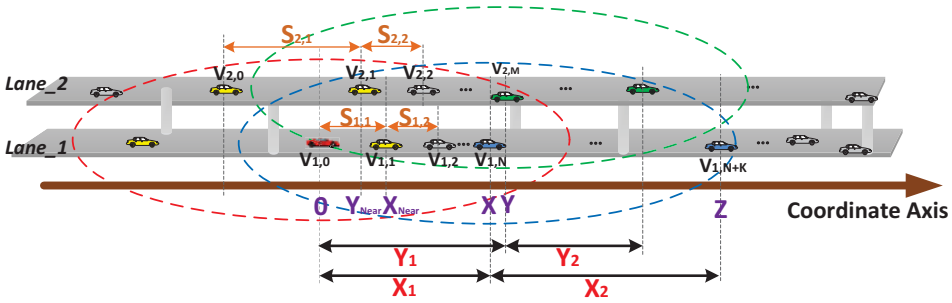

Fig. 2. The system model.

GF algorithm potentially induces a decrease on the delivery ratio in the multilevel VANET, because a bad inter-level neighbor is selected as the relay.

In the following, we will give our system model and prove the issues theoretically.

III. System Model and Problem Statement

In the section, we define notations, the problem statement and system model. Without loss of generality (W. L. O. G.), we consider a multilevel VANET composed of vehicles that are distributed in a two-level street. Major notions used in this paper are summarized in Table I.

A. System Model

The two-level scenario is extracted based on realistic traffic environments. Based on the scenario, our model is extracted as shown in Fig. 2. Two traffic flows exist in the model, where $Lane_1$ is on the lower-level and $Lane_2$ is on the upper-level. The two flows are independent from each other. The width of the street is much smaller than the transmission range such that the road can be taken as linear [18]. We number the jth node on $Lane_i$ by $V_{i,j}$, where j is an integer. W. L. O. G., we build a one-dimensional coordinate axis along the direction of the traffic flow with node $V_{1,0}$ as the reference. Drivers tend to maintain a constant spacing with their leader based on the car-following regime [33] [34]. Thus, we assume all vehicles have the same velocity v_i on $Lane_i$. The Poisson point process is used to model the node distribution. Let the inter-vehicle spacing between the node $V_{i,j-1}$ and $V_{i,j}$ be $S_{i,j}$. Then, the sequence $\{S_{i,j}\}$ is i.i.d. and $S_{i,j}$ follows the exponential distribution with density λ_i [18].

The communication model comes from [35]. A pair of vehicles can communicate if the distance between them is smaller than the transmission range. We define the *transmission range* by the horizontal distance between the transmitter and the receiver. However, two kinds of communications exist in the network. Let the range of intra-level transmission be R and the inter-level range be $R^{'}$. Thus, two node can communicate with each other if and only if the horizontal distance between them is smaller than R when they are on the same-level, or smaller than $R^{'}$ when they are on different levels.

B. Problem Statement

The node distribution, communication mode and RSR all change in the multilevel VANET. These variations might impact the performance of geographic routing protocols which depends on the connectivity probability and GF algorithm. In this paper, we try to prove and response the impacts. In particular, we are interested in answering the following four questions.

Problem 1. Both the intra-level communication and the inter-level communication exist in the multilevel VANET. However, what is the relation of the two transmission ranges in the two communications? We can answer the question by comparing values of R and R'.

Problem 2. The network *connectivity probability* is described by the probability that a node cannot find an available neighbor. Then, does the multilevel structure have impact on the connectivity? Let the probability be C_{ideal} without considering the transmission range degradation (i.e., $R' = R$). The probability is C_{real} when we consider the degradation (i.e., $R' < R$). The question equals to find the relation of C_{ideal} and C_{real}.

Problem 3. Given the distance between the source and destination, the *average hop* is the average hops that a packet travels from its source to the destination. The *delivery ratio* is the ratio between the number of successfully received packets and the total number of packets. Compared with 2D VANETs, what is the variation of the two metrics on the GF algorithm in the multilevel VANET? Let the probability of the hop increase caused by GF be p_{Gh}, and the probability of the delivery ratio decrease be p_{Gd}. We try to solve the problem by derive expressions for p_{Gh} and p_{Gd}.

Problem 4. Can we handle these impacts on geographic routing protocols, if all above three questions

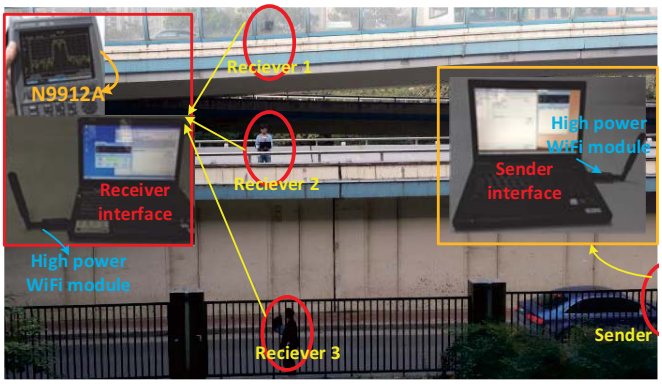

Fig. 3. Snapshot of the transmission experiment. Xi'an, China, Coordinates(34.23325, 108.92213)

have negative answers in the multilevel VANET?

IV. Impacts of the Multilevel Structure

This section concerns the first three problems. We execute an outdoor transmission experiment to measure the two transmission ranges for the first problem. Furthermore, we focus on problem 2 and 3, and make a stochastic analysis for the performance of the existing geographic routing protocol.

A. On Transmission Range

We execute the transmission experiment [32] on Taibai Interchange in Xi'an with latitude and longitude $(34.23325, 108.92213)$. Fig. 3 shows a snapshot of the experiment environment. The interchange is a three-level interchange. Respecting to the lowest level, heights of the two upper levels are 6 meters and 10 meters respectively.

Composed of a laptop, a GPS device and a high power WiFi module, the sender delivers packets continuously during the experiment. In addition to the same equipments of the sender, the receiver use a N9912A FieldFox handhold BF combination analyzer to detect the received power. We measure the distance between the receiver and the sender when they can normally communicate (R_D), as well as the distance that the two nodes can connect to each other but can not realize the normal communication (R_C). We test the two distances in three scenarios and on two frequency bands, i.e., 2.4G and 5.9G. The statistical average results are shown in Table II.

The first scenario is a 2D scenario, in which both the sender and receiver are on the same level. Only the intra-level communication occurs in the scenario. Test results are shown in the third and fourth rows. In the 3D(6m) scenario, the two nodes are on the lowest level and middle level respectively, while they are on the lowest level and highest one separately in the 3D(10m) scenario.

TABLE II
Test results of the transmission range

Scenario	Type	2.4G		5.9G	
		Data	$\delta(\%)$	Data	$\delta(\%)$
2D	R_{Data}	144	-	139.5	-
	R_{Conn}	202.05	-	179.18	-
3D(6m)	R_{Data}	89.75	62.3	51.5	36.9
	R_{Conn}	146	72.3	96.5	53.9
3D(10m)	R_{Data}	16.25	11.3	5	3.6
	R_{Conn}	50.45	25	38.3	21.4

The two 3D scenarios represent the case of the inter-level communication, whose results are given in the last four rows. In case of 5.9G, we compare results in 2D and two 3D scenarios. Taken results in the 2D scenario as references, the value of R_D is reduced by 60% in case of 3D(6m) and up to 90% in case of 3D(10m). This is because larger fading, path loss, noise and interference exist in inter-level communication. We get that the inter-level transmission range is much smaller than the intra-level communication range. The transmission range in 3D(6m) is bigger than that in 3D(10m), which means that the higher the inter-level spacing is, the higher the degradation of the inter-level transmission range is. In case of 2.4G, similar results can be concluded.

In particular, the transmission range dramatically changes with the highly dynamic traffic flow [9]. It makes channel modeling extremely complicated. However, this is out of our scope. Our experiments have revealed the existence and severity of the transmission range degradation. Therefore, we assume that the two transmission ranges follow $R' = \delta R$ in this paper, where δ is the transmission range degradation and satisfies $0 < \delta \leq 1$.

B. On Connectivity Probability

The connectivity probability is an important factor for the direction selection in geographic routing protocol. The wrong evaluation of the probability leads to a reduction of the routing performance. In this Section, we deduce closed-form expressions for C_{ideal} and C_{real}, which can reveal the variation of the connectivity probability in the multilevel VANET. According to the definition, the connectivity probability depends on the spacing between the reference node and its nearest node. Thus, it can be calculated if we have the distribution of the spacing. However, a node potentially has two kinds of neighbors in the network. It results in two kinds of spacings, which can be portrayed by the following lemma.

Lemma 1. *In the multilevel VANET, let the inter-vehicle spacing be exponentially distributed with the parameter*

λ_1 on $Lane_1$ and λ_2 on $Lane_2$ respectively. Let $R' = \delta R$, where $0 < \delta \leq 1$. Then, we have

(i) the CDF of the spacing between the reference node and its nearest intra-level node (i.e., X_{Near}) is given by

$$F_{X_{Near}}(x) = 1 - e^{-\lambda_1 x},\ x \in (0, \infty), \tag{1}$$

(ii) and the CDF of the spacing between the reference and its nearest inter-level node (i.e., Y_{Near}) is given by

$$F_{Y_{Near}}(y) = 1 - e^{-\lambda_2 y} - \lambda_2 y Ei(-\lambda_2 y),\ y \in (0, \infty). \tag{2}$$

Proof. (i) Immediately by the definition.

(ii) $V_{2,0}$ and $V_{2,1}$ are the nearest inter-level nodes of the reference $V_{1,0}$. Thus, $V_{1,0}$ can be seen as a node randomly distributed between $V_{2,0}$ and $V_{2,1}$ along the coordinate axis. The horizontal distance between $V_{1,0}$ and $V_{2,1}$ is Y_{Near}, which uniformly distributes in $(0, S_{2,1})$. Thus, the CDF of Y_{Near} is given by

$$\begin{aligned} F_{Y_{Near}}(y) &= \Pr\{Y_{Near} \leq y\} \\ &= \int_0^\infty \Pr\{Y_{Near} \leq y \,|S_{2,1} = s\} f_{S_{2,1}}(s)\, ds \\ &= \int_0^y \lambda_2 e^{-\lambda_2 s} ds + \int_y^\infty \frac{y}{s} \lambda_2 e^{-\lambda_2 s} ds \\ &= 1 - e^{-\lambda_2 y} - \lambda_2 y Ei(-\lambda_2 y),\ y \in (0, \infty). \end{aligned} \tag{3}$$

□

After deducing X_{Near} and Y_{Near}, we can evaluate C_{ideal} and C_{real}. Without considering the transmission degradation ($\delta = 1$), the connectivity is portrayed by C_{ideal}, where

$$\begin{aligned} C_{ideal} &= (1 - F_{X_{Near}}(R))(1 - F_{Y_{Near}}(R)) \\ &= e^{-\lambda_1 R}\left(e^{-\lambda_2 R} + \lambda_2 R Ei(-\lambda_2 R)\right). \end{aligned} \tag{4}$$

Taking the transmission degradation into consideration ($0 < \delta < 1$), the connectivity is changed to

$$\begin{aligned} C_{real} &= (1 - F_{X_{Near}}(R))(1 - F_{Y_{Near}}(R')) \\ &= e^{-\lambda_1 R}\left(e^{-\lambda_2 R'} + \lambda_2 R' Ei(-\lambda_2 R')\right). \end{aligned} \tag{5}$$

Furthermore, we have their difference by

$$\begin{aligned} C_{real} - C_{ideal} &= e^{-\lambda_1 R}\left(F_{Y_{Near}}(R) - F_{Y_{Near}}(R')\right) \\ &= e^{-\lambda_1 R}(R - R') f_{Y_{Near}}(\theta), \end{aligned} \tag{6}$$

in which $f_{Y_{Near}}(\theta)$ is the PDF of Y_{Near} and $\theta \in (R', R)$. Consequently, we have $C_{real} > C_{ideal}$, as well as a lower bound $e^{-\lambda_1 R}(1 - \delta)(-\lambda_2 R Ei(-\lambda_2 R))$ for the difference. Thus, the probability that a node cannot find an available neighbor grows if we consider the transmission range degradation. In other words, the degradation deteriorates the network connectivity. This remains us that the calculation method of connectivity probability should be reconsidered for geographic routing protocols in the multilevel VANET.

C. On GF Algorithm

The impacts of the multilevel structure on the GF algorithm are analyzed in this part. In particular, we calculate the probability of hop count increase (p_{Gh}) and delivery ratio decrease (p_{Gd}) to portray the variation of GF's performance. We denote the ith one-hop progress by a random variable X_i for the route on $Lane_1$, while Y_j depicts the jth one-hop progress for the route on $Lane_2$, where i and j are positive integers. We first need three important spacings, i.e., X_1, Y_1 and X_2, for analyzing the GF algorithm. For convenience, we replace X_1, Y_1 and X_2 with X, Y and Z respectively.

Lemma 2. *In the multilevel VANET, let the inter-vehicle spacing be exponentially distributed with the parameter λ_1 on $Lane_1$ and λ_2 on $Lane_2$ respectively. Let $R' = \delta R$, where $0 < \delta \leq 1$. Then, we have*

(i) the CDF of the spacing between the reference node and its furthest intra-level neighbor (i.e., X) is given by

$$F_X(x) = \frac{e^{-\lambda_1 R}\left(e^{\lambda_1 x} - 1\right)}{1 - e^{-\lambda_1 R}}, \tag{7}$$

(ii) the CDF of the spacing between the reference node and its furthest inter-level neighbor (i.e., Y) is given by

$$F_Y(y) = \frac{e^{-\lambda_2(R'-y)}\left(1 - e^{-\lambda_2 y} - \lambda_2 y Ei(-\lambda_2 y)\right)}{1 - e^{-\lambda_2 R'} - \lambda_2 R' Ei(-\lambda_2 R')}, \tag{8}$$

(iii) and the CDF of the 2nd one-hop progress on $Lane_1$ (i.e., Z) is described by

$$F_{Z|X}(z|x) = \frac{e^{\lambda_1(z-R)} - e^{-\lambda_1 x}}{1 - e^{-\lambda_1 x}}, \tag{9}$$

where $x \in (0, R)$, $y \in \left(0, R'\right)$ and $z \in (R - x, R)$.

Proof. (i) We portray the routing process of the GF algorithm by a renewal process, because distributions of inter-vehicle spacings are positive, independent, identically distributed, random variables. Let the number of the reference node's intra-level neighbors be N, where N is a nonnegative integer. Then, the value of X is equal to $X = \sum_{i=1}^{N} S_{1,i}$. We have $\sum_{i=1}^{N-1} S_{1,i} < X \leq R$ and $\sum_{i=1}^{N+1} S_{1,i} > R$. Let $N_{i,[a,b]}$ be the number of nodes in the range $[a, b]$ on $Lane_i$. Then, we can calculate the CDF of X by

$$
\begin{aligned}
F_X(x) &= \Pr(X \le x) \\
&= \Pr\left(\sum_{i=1}^{N} S_{1,i} \le x, \sum_{i=1}^{N+1} S_{1,i} > R \,|\, x \le R\right) \\
&= \frac{\sum_{n=1}^{\infty} \Pr\left(\sum_{i=1}^{n} S_{1,i} \le x, \sum_{i=1}^{n+1} S_{1,i} > R, x \le R\right)}{\Pr\{x \le R\}} \\
&= \frac{\sum_{n=1}^{\infty} \Pr\left(N_{1,[0,x]} = n\right) \Pr\left(N_{1,[x,R]} = 0\right)}{1 - e^{-\lambda_1 R}} \\
&= \frac{\sum_{n=1}^{\infty} \left(\frac{(\lambda_1 x)^n}{n!} e^{-\lambda_1 x}\right) e^{-\lambda_1 (R-x)}}{1 - e^{-\lambda_1 R}} \\
&= \frac{e^{-\lambda_1 R}\left(e^{\lambda_1 x} - 1\right)}{1 - e^{-\lambda_1 R}}, \quad x \in (0, R].
\end{aligned} \tag{10}
$$

(ii) Assume the reference node has M inter-level neighbors, where M is a nonnegative integer. Then, the distance between the reference and its furthest inter-level neighbor is given by $Y = \sum_{i=1}^{M} S_{2,i}$. We have $\sum_{i=1}^{M-1} S_{2,i} < Y \le R$ and $\sum_{i=1}^{M+1} S_{2,i} > R$. Thus, we can get the CDF of Y by

$$
\begin{aligned}
&F_Y(y) = \Pr\{Y \le y\} \\
&= \Pr\left\{\sum_{j=1}^{M} S_{2,j} \le y, \sum_{j=1}^{M+1} S_{2,j} > R' \,\middle|\, y \le R'\right\} \\
&= \frac{\int_0^y f_{Y_n}(s) \Pr\left\{\sum_{j=2}^{M} S_{2,j} \le y - s, \sum_{j=2}^{M+1} S_{2,j} > R' - s, y \le R'\right\} ds}{\Pr\left\{Y_n \le R'\right\}} \\
&= \frac{\int_0^y f_{Y_n}(s) \sum_{m=1}^{\infty} \Pr\left\{Z_{2,[0,y-s]} = m-1\right\} \Pr\left\{Z_{2,\left[y-s,R'\right]} = 0\right\} ds}{1 - \Pr\left\{Y_n > R'\right\}} \\
&= \frac{\int_0^y f_{Y_n}(s) \sum_{m=1}^{\infty} \left(\frac{(\lambda_2 (y-s))^{m-1}}{(m-1)!} e^{-\lambda_2 (y-s)}\right) e^{-\lambda_2 \left(R' - y + s\right)} ds}{1 - e^{-\lambda_2 R'} - \lambda_2 R' Ei\left(-\lambda_2 R'\right)} \\
&= \frac{e^{-\lambda_2 \left(R' - y\right)} \left(1 - e^{-\lambda_2 y} - \lambda_2 y Ei\left(-\lambda_2 y\right)\right)}{1 - e^{-\lambda_2 R'} - \lambda_2 R' Ei\left(-\lambda_2 R'\right)}, \; y \in \left(0, R'\right].
\end{aligned} \tag{11}
$$

(iii) In the GF algorithm, the relay is selected one by one. Therefore, the lth relay depends on the $(l-1)$th relay. Assume the first relay has K neighbors on $Lane_1$. Given the first one-hop progress on $Lane_1$ is X, the conditional distribution of the second one-hop progress on the same level Z can be calculated by

$$
\begin{aligned}
&F_{Z|X}(z|x) = \Pr(Z \le z | X = x) \\
&= \Pr\left(\sum_{j=N+1}^{N+K} S_{1,j} \le z, \sum_{j=N+1}^{N+K+1} S_{1,j} > R \,|\, R - x < z \le R\right) \\
&= \frac{\Pr\left(N_{1,[R,x+z]} = K\right) \Pr\left(N_{1,[x+z,x+R]} = 0\right)}{\Pr\left(N_{1,[R,x+R]} \ne 0\right)} \\
&= \frac{\sum_{k=1}^{\infty} \frac{(\lambda_1 (z-R+x))^k}{k!} e^{-\lambda_1 (z-R+x)} e^{-\lambda_1 (R-z)}}{1 - e^{-\lambda_1 x}} \\
&= \frac{e^{\lambda_1 (z-R)} - e^{-\lambda_1 x}}{1 - e^{-\lambda_1 x}}, \; z \in (R - x, R].
\end{aligned} \tag{12}
$$

□

Based on Lemma 2, we can immediately get the PDF of X and Y, and the conditional PDF of Z. Before evaluating the performance of GF, we need define two useful functions. Define the function $\phi(u)$ by

$$
\phi(u) = 1 - e^{-u} - u e^{-u}, \; u > 0. \tag{13}
$$

Define the function $\varphi(u, v)$ by

$$
\varphi(u, v) = 1 - e^{-u} - u e^{-v}, \; v \ge u > 0. \tag{14}
$$

Then, we have the property that $\varphi(u, v) = \phi(u) + u\left(e^{-u} - e^{-v}\right) \ge 0$.

1) On Hop Count: Compared with 2D VANETs, the GF algorithm shows a higher hop count with a probability in the multilevel VANET. We can theoretically analyze the probability by Theorem 1.

Theorem 1. *Compared with 2D VANETs, the hop increase probability of the GF algorithm induced by the multilevel structure (denoted by p_{Gh}) is given by*

$$
p_{Gh} = \frac{\Pr\{X_2 > Y_2, Y_1 > X_1\}}{\Pr\{Y_1 > X_1\}} > 0, \tag{15}
$$

where $\Pr\{X_2 > Y_2, Y_1 > X_1\}$ *is given by*

$$
\begin{aligned}
&\Pr\{X_2 > Y_2, Y_1 > X_1\} \\
&= \Pr\{R < 2R'\} \left(\beta E\left[e^{\lambda_1 Y} \phi\left(\left(\lambda_1 + \lambda_2\right) Y\right) | Y \le \Delta R\right]\right. \\
&+ \left.\beta \phi\left(\left(\lambda_1 + \lambda_2\right) \Delta R\right) E\left[e^{\lambda_1 Y} | Y > \Delta R\right]\right) \\
&+ \Pr\{R \ge 2R'\} \beta E\left[e^{\lambda_1 Y} \phi\left(\left(\lambda_1 + \lambda_2\right) Y\right)\right],
\end{aligned} \tag{16}
$$

$\Pr\{Y_1 > X_1\} = E[F_X(Y)]$, $\beta = \alpha(\lambda_1/(\lambda_1 + \lambda_2))^2$ *and* $\alpha = e^{-\lambda_1 R} / \left(1 - e^{-\lambda_1 R}\right)$.

Proof. See appendices A. □

2) On Delivery Ratio: In Section II, we have given a instance that the delivery ratio of the GF algorithm reduces in the multilevel VANET. To reveal the severity, we calculate the probability of the delivery decrease probability by theorem 2.

Theorem 2. *Compared with 2D VANETs, the delivery ratio decrease probability of the GF algorithm induced by the multilevel structure (denoted by p_{Gd}) is given by*

$$p_{Gd} = \frac{\Pr\{X_2 \neq 0, Y_2 = 0, Y_1 > X_1\}}{\Pr\{Y_1 > X_1\}} > 0, \quad (17)$$

where $\Pr\{X_2 \neq 0, Y_2 = 0, Y_1 > X_1\}$ *is given by the following expression*

$$\begin{aligned}
&\Pr\{X_2 \neq 0, Y_2 = 0, Y_1 > X_1\} \\
&= \Pr\left\{R < 2R'\right\}\left(\alpha e^{-\lambda_2 \Delta R} E\left[e^{(\lambda_1-\lambda_2)Y}\phi(\lambda_1 Y)\,|Y \leq \Delta R\right]\right. \\
&+ \left.\alpha e^{(\lambda_1-\lambda_2)\Delta R}\phi(\lambda_1 \Delta R)\, E\left[e^{-\lambda_2 Y}\,|Y > \Delta R\right]\right) \\
&+ \Pr\left\{R \geq 2R'\right\}\alpha e^{-\lambda_2 \Delta R} E\left[e^{(\lambda_1-\lambda_2)Y}\phi(\lambda_1 Y)\right].
\end{aligned} \quad (18)$$

Proof. See appendices B. □

The real data measured in our outdoor transmission experiment shows that the wireless transmission range has a degradation in the inter-level communication. Consequently, the degradation induces the deduction of the network connectivity, which impacts the direction selection at the intersection. Meanwhile, Theorem1 and 2 prove that the GF algorithm presents the issues of hop count increase and delivery ratio decrease in the multilevel VANET, which influences the forwarding on the road segment. Therefore, geographic routing protocols have performance degradations in the multilevel VANET. To address the issue, we give a solution in Section V.

V. The Proposed M-GOR

Motivated by the above results, we propose M-GOR for the multilevel VANET. In this section, we first give the details of the proposed protocol. Following the description, we analyze the issues of the hop count and delivery ratio for M-GOR.

A. The Proposed Protocol

We make the following assumptions in M-GOR. Location information is necessary for the routing decision, which is provided by GPS devices. The hello scheme and location management system are used for obtaining locations of neighbors and the destination [24]. All vehicles are equipped with preloaded digital maps providing the street-level map and traffic flow statistics, such as the traffic density and traffic signal schedule. The source is on $Lane_1$.

Algorithm 1 M-GOR

Input: Source and destination
Source initializes the routing process and inserts necessary information into the packet
$Transmitter_{id} = Source_{id}$
$hop = 1$
repeat
  if Transmitter touches destination by 1 hop **then**
    Transmit the packet to destination
    $Relay_{hop,id} = Destination_{id}$
    $Transmitter_{id} = Relay_{hop,id}$
  else
    if Transmitter is at an intersection **then**
      Enter the **Intersection Mode**
      Calculate weights for connecting segments
      Select a segment with the smallest weight
    end if
    Enter the **Segment Mode**
    if Transmitter has available neighbors **then**
      Using **GOF** to select the relay $Relay_{hop}$
    else if Within the packet lifetime **then**
      Transmitter carries the packet until it meets an available neighbor $Relay_{hop}$
    else
      Drop the packet
    end if
    Transmit the packet to $Relay_{hop}$
    $Transmitter_{id} = Relay_{hop,id}$
    $++hop$
  end if
until $Transmitter_{id} = Destination_{id}$
Output: $\{Source_{id}\} \cup \{\mathrm{R}ealy_{i,id}, i = 1, ..., hop\}$

The multilevel structure locates between the city and highway, which suffers both the issue of intermittent connection and the impact of the intersection. As a routing for the scenario, M-GOR considers the routing decision at the intersection and on the road segment separately to circumvent the unique challenge placed by the intersection. Therefore, two forwarding modes exist in the proposed protocol. A new calculation method for the connectivity probability is designed in the intersection mode, while we present a greedy opportunity forwarding (GOF) algorithm for the relay selection on the road segment. In particular, to deal with the issue of intermittent connection, we adopt the carry-and-forward algorithm when the transmitter has no available neighbors.

The process of M-GOR is shown in Algorithm 1. In the protocol, a source node initializes the process for a

packet delivery. For a transmitter, it checks its location for the first step. The intersection mode occurs when the transmitter locates on intersections. Depending on the location of itself and the destination, the transmitter chooses one direction for the delivery. Then, it turns to the segment mode for forwarding. The segment mode is used if the transmitter locates on road segments. According to the proposed GOF algorithm, the packet is transmitted hop by hop on the chosen direction. In particular, if there is no available neighbor, the transmitter will carry the packet until it touches an available relay. The process is repeated until the destination receives the packet. The details of the two modes are described as follows.

1) Intersection Mode: The intersection mode occurs if the transmitter joins an intersection. The transmitter will calculate weights for all connecting road segments and choose one with the smallest weight to transmit the packet. We consider both the distance and connectivity probability for the calculation. The weight is calculated based on the following equation [26]

$$\omega = \kappa D_{segment,destination} + (1-\kappa) C_{real}, \tag{19}$$

in which $D_{segment,destination}$ depicts the distance between the segment and destination, C_{real} is the defined connectivity probability of the segment, and $0 \leq \kappa \leq 1$ is the weight factor. However, considering the impacts of the multilevel structure, we define the distance by 3D Euclidean distance in M-GOR. Particularly, we calculate the connectivity probability based on Eq. 5.

2) Segment Mode: The segment mode always follows the intersection mode. In this mode, we present a GOF algorithm to select the next hop. The motivation of M-GOR is to increase the transmission opportunity of intra-level neighbors of the transmitter as much as possible. The transmitter is aware of all neighbors' locations by the hello scheme. Let the furthest intra-level neighbor be node V_{intra}, while the furthest inter-level neighbor is node V_{inter}. Let the distances between the current node and the two kinds of neighbors be X_1 and Y_1 respectively. The furthest inter-level neighbor V_{inter} is chosen as the next hop if and only if we have $Y_1 > X_1 + \sigma$, in which $\sigma = \begin{cases} (\lambda_1 - \lambda_2)\Delta R/\lambda_1 & \lambda_1 > \lambda_2 \\ 0 & \lambda_1 \leq \lambda_2 \end{cases}$. Otherwize, the packet is transmitted to node V_{intra}. In addition, we use the carry-and-forward algorithm as the recovery scheme if the transmitter has no valid neighbors. At this time, the transmitter will carry the packet until it meets an available node, or the lifetime of the packet exhausts.

Algorithm 2 The algorithm of GOF

1: **Input:** Transmitter, its furthest intra-level neighbor (V_{intra}) and its furthest inter-level neighbor (V_{inter})
2: **if** $D_{transmitter,V_{\text{inter}}} > D_{transmitter,V_{\text{intra}}} + \sigma$ **then**
3: V_{inter} is the next relay
4: **else**
5: V_{intra} is the next relay
6: **end if**
7: **Output:** The next relay

B. Theoretical Analysis of GOF

We give the theoretical analysis for the issues of hop count increase and delivery ratio decrease of the proposed GOF algorithm. By Lemma 2, we get the PDF of the one-hop progress on both levels described by $f_X(x)$ and $f_Y(y)$. Given the first one-hop progress X, we get the conditional PDF of the second one-hop progress on $Lane_1$ by $f_{Z|X}(z)$. For comparison, we analyze the same metrics for GOF with GF, i.e., the variation of the hop count and delivery ratio. The two values are portrayed by Theorem 3 and 4, respectively.

Theorem 3. *Compared with 2D VANETs, the hop increase probability of the GOF algorithm in the multilevel VANET (denoted by p_{Th}) is given by*

$$p_{Th} = \frac{\Pr\{X_2 > Y_2, Y_1 > X_1 + \sigma\}}{\Pr\{Y_1 > X_1 + \sigma\}}, \tag{20}$$

in which

$$\begin{aligned} &\Pr\{X_2 > Y_2, Y_1 > X_1 + \sigma\} \\ &= \Pr\{R < 2R'\}\beta\left(E\left[e^{\lambda_1 Y}\ (\phi((\lambda_1+\lambda_2)Y)\right.\right. \\ &\left.-\varphi(\sigma(\lambda_1+\lambda_2),(\lambda_1+\lambda_2)Y))\,|\sigma < Y \leq \Delta R\right] \\ &+ E\left[e^{\lambda_1 Y}\,|Y > \Delta R\right](\phi((\lambda_1+\lambda_2)\Delta R) \\ &\left.-\varphi(\sigma(\lambda_1+\lambda_2),(\lambda_1+\lambda_2)\Delta R))\right) \\ &+ \Pr\{R \geq 2R'\}\beta E\left[e^{\lambda_1 Y}(\phi((\lambda_1+\lambda_2)Y)\right. \\ &\left.-\varphi(\sigma(\lambda_1+\lambda_2),(\lambda_1+\lambda_2)Y))\,|\sigma < Y \leq R'\right], \end{aligned} \tag{21}$$

and $\Pr\{Y_1 > X_1 + \sigma\} = E[F_X(Y-\sigma)\,|Y > \sigma]$.

Proof. See appendices C. □

Theorem 4. *Compared with 2D VANETs, the delivery ratio decrease probability of the GOF algorithm in the multilevel VANET (denoted by p_{Td}) is given by*

$$p_{Td} = \frac{\Pr\{X_2 \neq 0, Y_2 = 0, Y_1 > X_1 + \sigma\}}{\Pr\{Y_1 > X_1 + \sigma\}}, \tag{22}$$

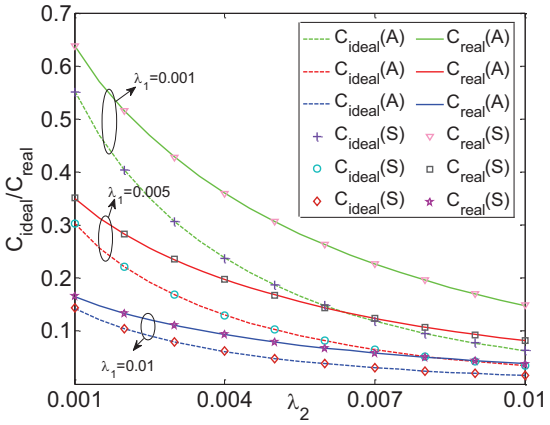

Fig. 4. Connectivity V. S. Node density

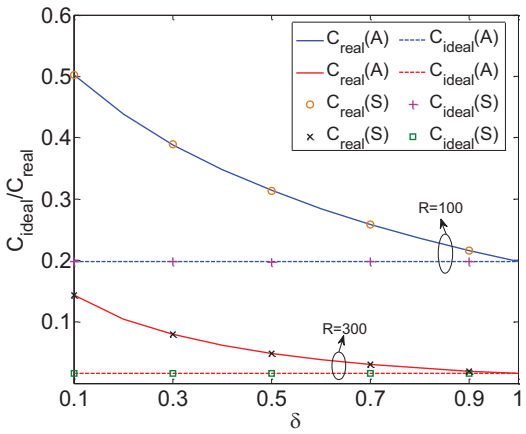

Fig. 5. Connectivity V. S. Transmission degradation

where $\Pr\{X_2 \neq 0, Y_2 = 0, Y_1 > X_1 + \sigma\}$ *is given by*

$$\begin{aligned}&\Pr\{X_2 \neq 0, Y_2 = 0, Y_1 > X_1 + \sigma\}\\&= \Pr\{R < 2R'\}\,\alpha\Big(e^{(\lambda_1-\lambda_2)\Delta R}E\left[e^{-\lambda_2 Y}\,|Y > \Delta R\right]\\&\times\left(\phi\left(\lambda_1\Delta R\right) - \varphi\left(\sigma\lambda_1, \lambda_1\Delta R\right)\right) + e^{-\lambda_2\Delta R}\\&\times E\left[e^{(\lambda_1-\lambda_2)Y}\left(\phi\left(\lambda_1 Y\right) - \varphi\left(\sigma\lambda_1, \lambda_1 Y\right)\right)|\sigma < Y \leq \Delta R\right]\Big)\\&+ \Pr\{R \geq 2R'\}\,\alpha e^{-\lambda_2\Delta R}E\big[e^{(\lambda_1-\lambda_2)Y}\left(\phi\left(\lambda_1 Y\right)\right.\\&\left.-\varphi\left(\sigma\lambda_1, \lambda_1 Y\right)\right)\big|\sigma < Y \leq R'\big].\end{aligned} \tag{23}$$

Proof. See appendices D. □

Consequently, we have $p_{Th} < p_{Gh}$ and $p_{Td} < p_{Gd}$, which means that the GOF algorithm provides better performance in terms of the average hop count and delivery ratio than the GF algorithm in the multilevel VANET. Here, we have proved the effectiveness of the proposed GOF algorithm theoretically. Then, we will demonstrate the results by simulations.

VI. Simulation

A. Simulation Setup

To verify the analysis and performance of the proposed protocol, we conduct two types of simulations. First of all, we make Monte-Carlo simulations on the network layer to verify analysis results. The simulation environment is a two-level street which is similar to the scenario in Fig. 2. Results are shown from Fig. 4 to Fig.9. In addition, we conduct a system level simulation for M-GOR on the network simulator NS-2.34 [36]. In the simulation, GPCR [4] and GyTAR [26] are selected for comparison, because they are two of the most famous protocols and always chosen for comparison [37] [38]. The simulation is made in a $2500m \times 1500m$ street area, which covers 9 intersections and 2 viaducts. We get the multilevel mobility model by modifying the IDM model in mobility traces generator VanetMobiSim [39]. The MAC layer protocol follows 802.11p. We define $R = 250m$ and $R' = 200m$. The node number is varying from 60 to 200, which means that the node density of the multilevel network changes from 0.006 to 0.019. Ten nodes are randomly selected as data sources. The simulation time is 250s.

B. Results and Discussion

1) Performance Analysis on Network Layer: These results are given from Fig. 4 to 9. In these figures, all curves describe analysis results while markers depict simulation results. All the six figures show that our analysis results are in fact quite accurate.

In Fig. 4 and 5, we give the results for the connectivity probability. We portray the connectivity by the probability that a node cannot find a neighbor. The probability is denoted by C_{ideal} (when $\delta = 1$) and C_{real} (when $0 < \delta < 1$). Fig. 4 depicts the probability varying with the node density when we fix $R = 150$ and $R' = 90$. The results for $\lambda_1 = 0.001$, $\lambda_1 = 0.005$ and $\lambda_1 = 0.01$ are described by the green, red and blue lane respectively. C_{real} is much larger than C_{ideal} in the multilevel VANET. It means that the defined real connectivity probability is larger than that without considering the transmission degradation in the multilevel VANET. According to the analysis, the difference of the probability is bigger than $e^{-\lambda_1 R}\left(1-\delta\right)\left(-\lambda_2 REi\left(-\lambda_2 R\right)\right)$. The reason is the transmission range has a degradation in the network, which causes the reduction of RSR and then impacts the connectivity probability. Thus, the connectivity probability is overstated if the multilevel feature is ignored. Then, the performance of the routing decision is poor. Fig. 4 also reveals that the defined connectivity probability increases with the node density.

Let λ_1 and λ_2 be 0.004. Then, we reveal the variation of the connectivity probability caused by the transmis-

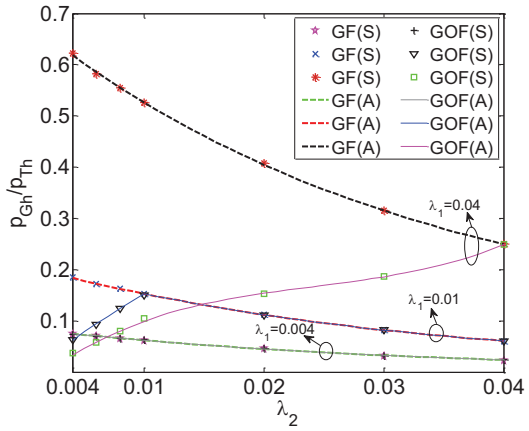

Fig. 6. Hop increase probability V. S. Node density

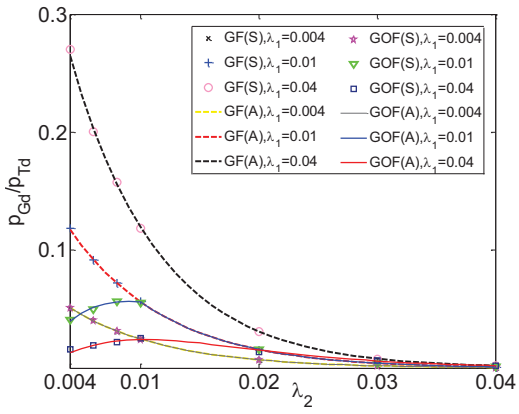

Fig. 8. Delivery decrease probability V. S. Node density

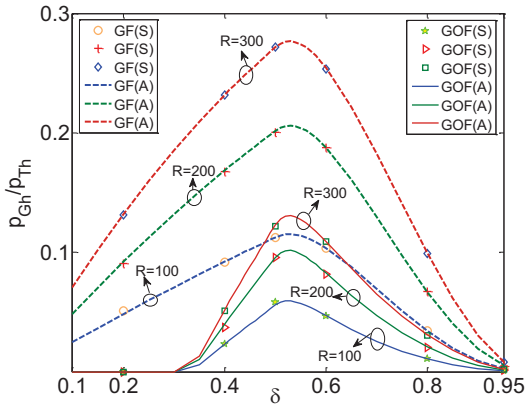

Fig. 7. Hop increase probability V. S. Transmission degradation

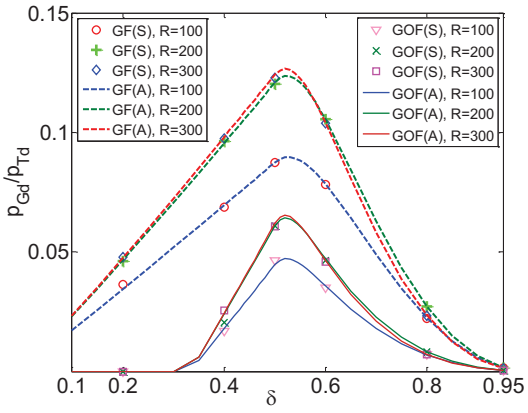

Fig. 9. Delivery decrease probability V. S. Transmission degradation

sion degradation in Fig. 5. In spite of the variation of R', C_{ideal} shows a constant value with fixed R. The reason is that the calculation method of C_{ideal} ignores the transmission degradation. However, C_{real} decreases with the degradation of the transmission range(that denoted by δ), which means that the defined connectivity probability decreases with δ. When $R = 100$, the value of C_{real} decreases from 0.5 to 0.2. The value changed from 0.14 to 0.02 when $R = 300$. It shows that the real connectivity probability are significantly impacted by δ. Therefore, we obtain that the existence of the multilevel structure severely impacts the network connectivity.

The issues of hop increase for the available GF algorithm and the proposed GOF algorithm are depicted in Fig. 6 and 7. Let R be 150 and R' be 90. Then, the results for the probability of hop count increase are given in Fig. 6. For $\lambda_1 = 0.004$, GOF has the same value of the probability with GF when λ_2 increases. The reason is that λ_2 varies from 0.004 to 0.04, which is always smaller than λ_1. Thus, the node density of the lower level is smaller than that of the upper level. Then, the transmitter will select the neighbor who makes the longest progress as the next hop in the GOF algorithm, which is same as the GF algorithm. When $\lambda_1 = 0.01$, the value of GOF is smaller than the GF algorithm when $\lambda_2 < \lambda_1 = 0.01$. This is because GOF selects the relay who can find neighbors with high probability. When $\lambda_2 > \lambda_1 = 0.01$, the results for the two algorithms are the same. Furthermore, the value of GOF is always smaller than the GF algorithm when $\lambda_1 = 0.04 > \lambda_2$. The GOF always has better performance if the level of the transmitter shows a higher node density.

Let λ_1 be 0.008 and λ_2 be 0.004. Then, we give the results for the hop increase probability varying with the transmission degradation in Fig. 7. In spite of the value of R, the GOF algorithm provides a lower hop increase probability than that of the GF algorithm. Moreover, all results of the probability for the two algorithms first increase and then decrease with δ, which shows that we can find upper bounds for the impacts of the transmission degradation on both algorithms. These bounds can be derived by Eq. 15 and Eq. 20.

The issues of delivery ratio decrease for the two algorithms are depicted in Fig. 8 and 9. Let R be 150 and

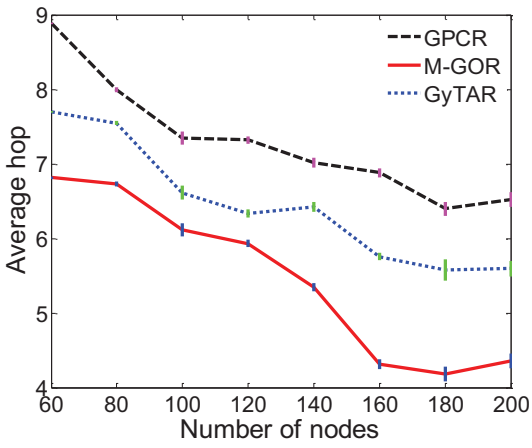

Fig. 10. Average hops V.S. node number.

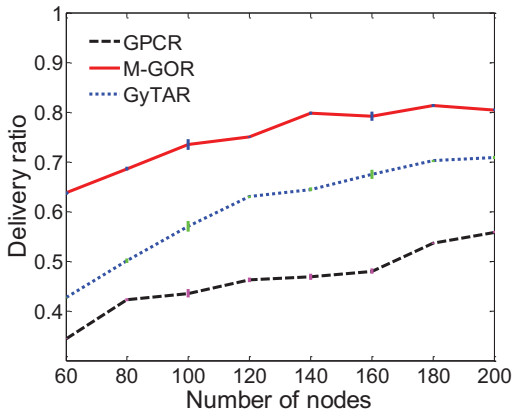

Fig. 11. Delivery ratio V.S. node number.

R' be 90. Then, we depict the probability of the delivery ratio decrease varying with λ_2 in Fig. 8. For each case, i.e., λ_1 = 0.004, 0.01 and 0.04, the probability of the GF algorithm decreases with λ_2. However, the value of GOF is smaller than GF algorithm when $\lambda_1 > \lambda_2$. The values of the two algorithms are the same when $\lambda_1 < \lambda_2$. The reason is that the GOF has advantage when the same level of the transmitter has a higher node density than other levels.

Let λ_1 be 0.008 and λ_2 be 0.004. Fig. 9 shows the probability of the delivery ratio varying with the degradation of the transmission range. In the figure, we get that the probability first increases and then decreases with δ for both of the algorithms in spite of the value of R. This means that the issue of the delivery ratio decrease is the most serious when the transmission range has about a half degradation. With the same R, GOF shows a smaller probability to drop a packet than the greedy forwarding algorithm. It is coincide with the analysis results.

2) Performance Analysis on System Level: In Fig. 10, we give results for the average hop count from the system simulation. Vertical lines represent the 95% confidence intervals of the simulation. The proposed M-GOR has the lowest hop count, which reveals M-GOR is more suitable than GyTAR and GPCR in the multilevel VANET. For each protocol, the higher the node density is, the lower the average hop count is. The reason is that the selected next-hop is coming closer to the transmission range boundary of the current node with the increasing node density. Thus, the hop count decreases. Fig. 10 reveals that the multilevel structure has the least influence on the hop count of M-GOR, which coincides with results in Fig. 6 and Fig. 7.

Fig. 11 portrays results of the delivery ratio. We also give the 95% confidence interval using vertical lines. It is observed in Fig. 12 that the delivery ratio of M-GOR increases from 63.9% to 80.5% which is always higher than GyTAR and GPCR. The reason is that M-GOR can find a suitable route using the greedy opportunistic forwarding algorithm in multilevel scenarios. With the increasing node density, the connectivity probability of the network is getting better. That is why the delivery ratio of all protocols increases. The value of M-GOR is the lowest, which means the influence of multilevel scenarios on the delivery ratio of M-GOR is the least. The results coincide with the theoretical results.

VII. Conclusion

This paper has investigated the geographic routing protocol for the multilevel VANET. We have revealed impacts of the multilevel structure by an outdoor transmission experiment and a stochastic analysis. The measured data has indicated that the wireless transmission range showed a dramatic degradation in the inter-level communication. Moreover, we have proved that the connectivity probability decreased without considering the degradation in the multilevel VANET (at least $e^{-\lambda_1 R}(1-\delta)(-\lambda_2 REi(-\lambda_2 R))$ in a two-level VANET). In addition, the GF algorithm based routing protocols suffer significant performance reductions in terms of the hop count and delivery ratio. Motivated by the above results, we have proposed M-GOR, in which we have presented a new calculation method for the connectivity probability and a GOF algorithm to respond these impacts. Finally, we have conducted simulations from both the network layer and system level. The results have verified the accuracy of our analysis, and showed that M-GOR gained up to 20% increase on the delivery ratio and 10% decrease on the average hop count.

In future, we will do formula deviation for the hop, delivery ratio and delay for routing protocols in the

multilevel VANET. Furthermore, we will consider the issue of routing in more complex and common 3D scenarios of VANETs.

APPENDIX A
PROOF OF THEOREM 1

We have

$$p_{Gh} = \Pr\{X_2 > Y_2 \,|Y_1 > X_1\} = \frac{\Pr\{X_2 > Y_2, Y_1 > X_1\}}{\Pr\{Y_1 > X_1\}}. \tag{24}$$

It is easy to get the expression of $\Pr\{Y_1 > X_1\}$ by

$$\begin{aligned}\Pr\{Y_1 > X_1\} &= \int_0^{R'}\int_0^{y} f_Y(y) f_X(x)\, dxdy \\ &= \int_0^{R'} f_Y(y) F_X(y)\, dy = E[F_X(Y)].\end{aligned} \tag{25}$$

To evaluate $\Pr\{X_2 > Y_2, Y_1 > X_1\}$, it has three cases.

Case 1: $Y > \Delta R$ when $R < 2R'$. Then,

$$\begin{aligned}p_{Gh1} &= \int_{\Delta R}^{R'}\int_{y-\Delta R}^{y}\int_{y+R'-x}^{R} f_Y(y) f_X(x) \\ &\times f_{Z|X}(z)\left(1-e^{-\lambda_1 x}\right)e^{-\lambda_2(y+R-x-z)}dzdxdy \\ &= \int_{\Delta R}^{R'} f_Y(y) e^{\lambda_1 y}\beta\phi\left((\lambda_1+\lambda_2)\Delta R\right)dy \\ &= \beta\phi\left((\lambda_1+\lambda_2)\Delta R\right)E\left[e^{\lambda_1 Y}\,|Y > \Delta R\right].\end{aligned} \tag{26}$$

Case 2: $Y \le \Delta R$ when $R < 2R'$. Then,

$$\begin{aligned}p_{Gh2} &= \int_0^{\Delta R}\int_0^{y}\int_{R-x}^{R} f_Y(y) f_X(x) f_{Z|X}(z) \\ &\times\left(1-e^{-\lambda_1 x}\right)e^{-\lambda_2(y+R-x-z)}dzdxdy \\ &= \int_0^{\Delta R} f_Y(y)\,\beta e^{\lambda_1 y}\phi\left((\lambda_1+\lambda_2)y\right)dy \\ &= \beta E\left[e^{\lambda_1 Y}\phi\left((\lambda_1+\lambda_2)Y\right)|Y \le \Delta R\right].\end{aligned} \tag{27}$$

Case 3: When $R \ge 2R'$, we have

$$\begin{aligned}p_{Gh3} &= \int_0^{R'}\int_0^{y}\int_{R-x}^{R} f_Y(y) f_X(x) f_{Z|X}(z) \\ &\times\left(1-e^{-\lambda_1 x}\right)e^{-\lambda_2(y+R-x-z)}dzdxdy \\ &= \int_0^{R'} f_Y(y)\,\beta e^{\lambda_1 y}\phi\left((\lambda_1+\lambda_2)y\right)dy \\ &= \beta E\left[e^{\lambda_1 Y}\phi\left((\lambda_1+\lambda_2)Y\right)\right].\end{aligned} \tag{28}$$

By submitting Eq. 25-28 to Eq. 24, Theorem 1 holds.

APPENDIX B
PROOF OF THEOREM 2

Since

$$\begin{aligned}p_{Gd} &= \Pr\{X_2 \ne 0, Y_2 = 0\,|Y_1 > X_1\} \\ &= \frac{\Pr\{X_2 \ne 0, Y_2 = 0, Y_1 > X_1\}}{\Pr\{Y_1 > X_1\}},\end{aligned} \tag{29}$$

there are three cases to get the value of $\Pr\{X_2 \ne 0, Y_2 = 0, Y_1 > X_1\}$.

Case 1: $Y > \Delta R$ when $R < 2R'$. Then,

$$\begin{aligned}p_{Gd2} &= \int_{\Delta R}^{R'}\int_{y-\Delta R}^{y}\int_{y+R'-x}^{R} f_Y(y) f_X(x) f_{Z|X}(z) \\ &\times\left(1-e^{-\lambda_1 x}\right)e^{-\lambda_2\left(y+R-R'\right)}e^{-\lambda_1\left(y+R'-R\right)}dzdxdy \\ &= \int_{\Delta R}^{R'} f_Y(y)\, e^{-\lambda_2 y}c_1 e^{(\lambda_1-\lambda_2)\Delta R}\beta(\lambda_1\Delta R)dy \\ &= \alpha e^{(\lambda_1-\lambda_2)\Delta R}\phi(\lambda_1\Delta R)\,E\left[e^{-\lambda_2 Y}\,|Y > \Delta R\right].\end{aligned} \tag{30}$$

Case 2: $Y \le \Delta R$ when $R < 2R'$. Then,

$$\begin{aligned}p_{Gd1} &= \int_0^{\Delta R}\int_0^{y}\int_{R-x}^{R} f_Y(y) f_X(x) f_{Z|X}(z) \\ &\times\left(1-e^{-\lambda_1 x}\right)e^{-\lambda_2\left(y+R-R'\right)}dzdxdy \\ &= \int_0^{\Delta R} f_Y(y)\, c_1 e^{-\lambda_2\Delta R}e^{(\lambda_1-\lambda_2)y}\beta(\lambda_1 y)dy \\ &= \alpha e^{-\lambda_2\Delta R}E\left[e^{(\lambda_1-\lambda_2)Y}\phi(\lambda_1 Y)\,|Y \le \Delta R\right].\end{aligned} \tag{31}$$

Case 3: When $R \ge 2R'$, we have

$$\begin{aligned}p_{Gd3} &= \int_0^{R'}\int_0^{y}\int_{R-x}^{R} f_Y(y) f_X(x) f_{Z|X}(z) \\ &\times\left(1-e^{-\lambda_1 x}\right)e^{-\lambda_2\left(y+R-R'\right)}dzdxdy \\ &= \int_0^{R'} f_Y(y)\, c_1 e^{-\lambda_2\Delta R}e^{(\lambda_1-\lambda_2)y}\beta(\lambda_1 y)dy \\ &= \alpha e^{-\lambda_2\Delta R}E\left[e^{(\lambda_1-\lambda_2)Y}\phi(\lambda_1 Y)\right].\end{aligned} \tag{32}$$

By submitting Eq. 30-32 to Eq. 29, Theorem 2 holds.

APPENDIX C
PROOF OF THEOREM 3

We have

$$\begin{aligned}p_{Th} &= \Pr\{X_2 > Y_2\,|Y_1 > X_1 + \sigma\} \\ &= \frac{\Pr\{X_2 > Y_2, Y_1 > X_1 + \sigma\}}{\Pr\{Y_1 > X_1 + \sigma\}}.\end{aligned} \tag{33}$$

It is easy to get the expression of $\Pr\{Y_1 > X_1 + \sigma\}$.

$$\begin{aligned}\Pr\{Y_1 > X_1 + \sigma\} &= \int_{\sigma}^{R'}\int_0^{y-\sigma} f_Y(y) f_X(x)\, dxdy \\ &= \int_{\sigma}^{R'} f_Y(y) F_X(y-\sigma)\, dy.\end{aligned} \tag{34}$$

To evaluate $\Pr\{X_2 > Y_2, Y_1 > X_1 + \sigma\}$, there are three cases.

Case 1: $Y > \Delta R$ when $R < 2R'$. Then,

$$\begin{aligned}p_{Th1} &= \int_{\Delta R}^{R'}\int_{y-\Delta R}^{y-\sigma}\int_{y+R'-x}^{R} f_Y(y) f_X(x) f_{Z|X}(z) \\ &\times\left(1-e^{-\lambda_1 x}\right)e^{-\lambda_2(y+R-x-z)}dzdxdy \\ &= \int_{\Delta R}^{R'} f_Y(y)\, e^{\lambda_1 y}\beta\left(\phi\left((\lambda_1+\lambda_2)\Delta R\right)\right. \\ &\left.-\varphi\left(\sigma(\lambda_1+\lambda_2), (\lambda_1+\lambda_2)\Delta R\right)\right)dy \\ &= \beta E\left[e^{\lambda_1 Y}\,|Y > \Delta R\right]\left(\phi\left((\lambda_1+\lambda_2)\Delta R\right)\right. \\ &\left.-\varphi\left(\sigma(\lambda_1+\lambda_2), (\lambda_1+\lambda_2)\Delta R\right)\right).\end{aligned} \tag{35}$$

Case 2: $Y \leq \Delta R$ when $R < 2R'$. Then,

$$\begin{aligned} p_{Th2} &= \int_{\sigma}^{\Delta R}\int_{0}^{y-\sigma}\int_{R-x}^{R} f_Y(y) f_X(x) f_{Z|X}(z) \\ &\times \left(1-e^{-\lambda_1 x}\right) e^{-\lambda_2(y+R-x-z)} dz dx dy \\ &= \int_{\sigma}^{\Delta R} f_Y(y) \beta e^{\lambda_1 y} \left(e^{\lambda_1 y}\phi\left((\lambda_1+\lambda_2)y\right)\right. \\ &\left.-\varphi\left(\sigma(\lambda_1+\lambda_2),(\lambda_1+\lambda_2)y\right)\right) dy \\ &= \beta E\left[e^{\lambda_1 Y}\left(\phi\left((\lambda_1+\lambda_2)Y\right)\right.\right. \\ &\left.\left.-\varphi\left(\sigma(\lambda_1+\lambda_2),(\lambda_1+\lambda_2)Y\right)\right)|\sigma < Y \leq \Delta R\right]. \end{aligned} \tag{36}$$

Case 3: When $R \geq 2R'$, we have

$$\begin{aligned} p_{Th3} &= \int_{\sigma}^{R'}\int_{0}^{y-\sigma}\int_{R-x}^{R} f_Y(y) f_X(x) f_{Z|X}(z) \\ &\times \left(1-e^{-\lambda_1 x}\right) e^{-\lambda_2(y+R-x-z)} dz dx dy \\ &= \int_{\sigma}^{R'} f_Y(y) \beta e^{\lambda_1 y} \left(e^{\lambda_1 y}\phi\left((\lambda_1+\lambda_2)y\right)\right. \\ &\left.-\varphi\left(\sigma(\lambda_1+\lambda_2),(\lambda_1+\lambda_2)y\right)\right) dy \\ &= \beta E\left[e^{\lambda_1 Y}\left(\phi\left((\lambda_1+\lambda_2)Y\right)\right.\right. \\ &\left.\left.-\varphi\left(\sigma(\lambda_1+\lambda_2),(\lambda_1+\lambda_2)Y\right)\right)|\sigma < Y \leq \Delta R\right]. \end{aligned} \tag{37}$$

By submitting Eq. 34-37 to Eq. 33, Theorem 3 holds.

Appendix D
Proof of Theorem 4

Since

$$\begin{aligned} p_{Td} &= \Pr\left\{X_2 \neq 0, Y_2 = 0 \,|Y_1 > X_1 + \sigma\right\} \\ &= \frac{\Pr\left\{X_2 \neq 0, Y_2 = 0, Y_1 > X_1 + \sigma\right\}}{\Pr\left\{Y_1 > X_1 + \sigma\right\}}, \end{aligned} \tag{38}$$

there are three cases to get the value of $\Pr\left\{X_2 \neq 0, Y_2 = 0, Y_1 > X_1 + \sigma\right\}$.

Case 1: $Y > \Delta R$ when $R < 2R'$. Then,

$$\begin{aligned} p_{Td1} &= \int_{\Delta R}^{R'}\int_{y-\Delta R}^{y-\sigma}\int_{y+R'-x}^{R} f_Y(y) f_X(x) f_{Z|X}(z) \\ &\times \left(1-e^{-\lambda_1 x}\right) e^{-\lambda_2\left(y+R-R'\right)} e^{-\lambda_1\left(y+R'-R\right)} dz dx dy \\ &= \alpha e^{(\lambda_1-\lambda_2)\Delta R}\left(\phi(\lambda_1\Delta R) - \varphi(\sigma\lambda_1, \lambda_1\Delta R)\right) \\ &\times \int_{\Delta R}^{R'} e^{-\lambda_2 y} f_Y(y) dy \\ &= \alpha e^{(\lambda_1-\lambda_2)\Delta R}\left(\phi(\lambda_1\Delta R) - \varphi(\sigma\lambda_1, \lambda_1\Delta R)\right) \\ &\times E\left[e^{-\lambda_2 Y}\,|Y > \Delta R\right]. \end{aligned} \tag{39}$$

Case 2: $Y \leq \Delta R$ when $R < 2R'$. Then,

$$\begin{aligned} p_{Td2} &= \int_{\sigma}^{\Delta R}\int_{0}^{y-\sigma}\int_{R-x}^{R} f_Y(y) f_X(x) f_{Z|X}(z) \\ &\times \left(1-e^{-\lambda_1 x}\right) e^{-\lambda_2\left(y+R-R'\right)} dz dx dy \\ &= \alpha e^{-\lambda_2\Delta R}\int_{\sigma}^{\Delta R} f_Y(y) e^{(\lambda_1-\lambda_2)y} \\ &\times \left(e^{-\lambda_1\sigma} - e^{-\lambda_1 y} - \lambda_1(y-\sigma)e^{-\lambda_1 y}\right) dy \\ &= \alpha e^{-\lambda_2\Delta R} E\left[e^{(\lambda_1-\lambda_2)Y}\left(\phi(\lambda_1 Y)\right.\right. \\ &\left.\left.-\varphi(\sigma\lambda_1, \lambda_1 Y)\right)|\sigma < Y \leq \Delta R\right]. \end{aligned} \tag{40}$$

Case 3: If $R \geq 2R'$, we have

$$\begin{aligned} p_{Td3} &= \int_{\sigma}^{R'}\int_{0}^{y-\sigma}\int_{R-x}^{R} f_Y(y) f_X(x) f_{Z|X}(z) \\ &\times \left(1-e^{-\lambda_1 x}\right) e^{-\lambda_2\left(y+R-R'\right)} dz dx dy \\ &= \alpha e^{-\lambda_2\Delta R}\int_{\sigma}^{R'} f_Y(y) e^{(\lambda_1-\lambda_2)y} \\ &\times \left(e^{-\lambda_1\sigma} - e^{-\lambda_1 y} - \lambda_1(y-\sigma)e^{-\lambda_1 y}\right) dy \\ &= \alpha e^{-\lambda_2\Delta R} E\left[e^{(\lambda_1-\lambda_2)Y}\left(\phi(\lambda_1 Y)\right.\right. \\ &\left.\left.-\varphi(\sigma\lambda_1, \lambda_1 Y)\right)\Big|\sigma < Y < R'\right]. \end{aligned} \tag{41}$$

By submitting Eq. 39-41 to Eq. 38, Theorem 4 holds.

References

[1] M. Alsabaan, W. Alasmary, A. Albasir and K. Naik, "Vehicular networks for a greener environment: a survey," *IEEE Commun. Surv. Tut.*, vol. 15, no. 3, pp. 1372-1388, Sep. 2013.

[2] F. Dressler, M. Gerla, O. Altintas, H. Hartenstein, M. Gruteser, J. Gozalvez and J. Pereira, "Inter-vehicle Communication: Quo Vadis," *IEEE Commun. Mag.*, vol. 52, no. 6, pp. 170-177, Jun. 2014.

[3] B. Karp and H. Kung, "GPSR: greedy perimeter stateless routing for wireless networks," in *Proc. ACM/IEEE MobiCom*, 2000, Boston, pp. 243-254.

[4] C. Lochert, M. Mauve, H. FiiBler and H. Hartenstein, "Geographic routing in city scenarios," *ACM SIGMOBILE Mob. Comput. Commun. Rev.*, vol. 9, no. 1, pp. 69-72, Jan. 2005.

[5] J. Chang, Y. Li, W. Liao and I. Chang, "Intersection-based routing for urban vehicular communications with traffic-light considerations," *IEEE Wirel. Commun.*, vol. 19, no. 1, pp. 82-88, Feb. 2012.

[6] H. Zhou, B, Liu, T. Luan, F. Hou, L. Gui, Y. Li, Q. Yu and X. Shen, "ChainCluster: engineering a cooperative content distribution framework for highway vehicular communications," *IEEE Trans. Intell. Transp. Syst.*, vol. 15, no. 6, pp. 2644-2657, May 2014.

[7] J. Cheng, J. Cheng, M. Zhou, F. Liu, S. Gao and C. Liu, "Routing in internet of vehicles: a review," *IEEE Trans. Intell. Transp. Syst.*, vol. pp, no. 99, pp.1-14, Mar. 2015.

[8] R. Zhang and L. Cai, "Joint AMC and packet fragmentation for error control over fading channels," *IEEE Trans. Veh. Technol.*, vol. 59, no. 6, pp. 3070-3080, Mar. 2010.

[9] M. Boban, T. Vinhoza, M. Ferreira, J. Barros and O. Tonguz, "Impact of vehicles as obstacles in vehicular ad hoc networks," *IEEE J. Sel. Areas Commun.*, vol. 29, no. 1, pp. 15-28, Jan. 2011.

[10] A. Banaei, D. Cline, C. Georghiades and S. Cui, "On asymptotic statistics for geometric routing schemes in wireless ad hoc networks," *IEEE/ACM Trans. Netw.*, vol. 23, no. 2, pp. 559 - 573, Apr. 2015.

[11] X. Wang, X. Lin, Q. Wang, W. Luan, "Mobility Increases the Connectivity of Wireless Networks," *IEEE/ACM Trans. Netw.*, vol. 21, no. 2, pp. 440-454, 2013.

[12] S. Ng, W. Zhang, Y. Zhang, Y. Yang and G. Mao, "Analysis of access and connectivity probabilities in vehicular relay networks," *IEEE J. Sel. Areas Commun.*, vol. 29, no. 1, pp. 140-150, Jan. 2011.

[13] Q. Lin, C. Li, X. Wang and L. Zhu, "A three-dimensional scenario oriented routing protocol in vehicular ad hoc networks," in *Proc. IEEE VTC Spring*, 2013, Dresden, pp. 1-5.

[14] S. Bitam, A. Mellouk and S. Zeadally, "Bio-inspired routing algorithms survey for vehicular ad hoc networks," *IEEE Commun. Surv. Tut.*, vol. 17, no. 2, pp. 843-867, May 2015.
[15] W. Sun, Z. Yang, K. Wang and Y. Liu, "Hello: a generic flexible protocol for neighbor discovery," in *Proc. IEEE INFOCOM*, 2014, Toronto, pp. 540-548.
[16] H. Saleet, O. Basir, R. Langar and R. Boutaba, "Region-based location-service-management protocol for vanets," *IEEE Trans. Veh. Technol.*, vol. 59, no. 2, pp. 917-931, Sep. 2009.
[17] P. Sahu, E. Wu, J. Sahoo and M. Gerla, "BAHG: back-bone-assisted hop greedy routing for VANET's city environments," *IEEE Trans. Intell. Transp. Syst.*, vol. 14, no. 1, pp. 199-213, Mar. 2013.
[18] T. Luan, X. Shen and F. Bai, "Integrity-oriented content transmission in highway vehicular ad hoc networks," in *Proc. IEEE INFOCOM*, 2013, Turin, pp. 2562-2570.
[19] N. Wisitpongphan, F. Bai, P. Mudalige, V. Sadekar and O. Tonguz, "Routing in sparse vehicular ad hoc wireless networks," *IEEE J. Sel. Areas Commun.*, vol. 25, no. 8, pp. 1538-1556, Oct. 2007.
[20] K. Abboud and W. Zhuang, "Stochastic analysis of single-hop communication link in vehicular ad hoc networks," in *IEEE Trans. Intell. Transp. Syst.*, vol. 15, no. 5, pp. 2297 - 2307, Oct. 2014.
[21] V. Namboodiri and L. Gao, "Prediction-based routing for vehicular ad hoc networks," *IEEE Trans. Veh. Technol.*, vol. 56, no. 4, pp. 2332-2345, Jul. 2007.
[22] V. Naumov and T. R. Gross, "Connectivity-aware routing (CAR) in vehicular ad hoc networks," in *Proc. IEEE INFOCOM*, 2007, Anchorage, pp. 1919-1927.
[23] N. Alsharif, S. Cespedes and X. Shen, "iCAR: intersection-based connectivity aware routing in vehicular networks," in *Proc. IEEE ICC*, 2013, Budapest, pp. 1736-1741.
[24] N. Alsharif and X. Shen, "iCARII: intersection-based connectivity aware routing in vehicular networks," in *Proc. IEEE ICC*, 2014, Sydney, pp. 2731 - 2735.
[25] Y. Ding, C. Wang and L. Xiao, "A static-node assisted adaptive routing protocol in vehicular networks," in *Proc. ACM VANET*, 2007, NY, USA, pp. 59-68.
[26] M. Jerbi, S. M. Senouci, T. Rasheed and Y. Ghamri-Doudane, "Towards efficient geographic routing in urban vehicular networks," *IEEE Trans. Veh. Technol.*, vol. 58, no. 9, pp. 5048-5059, Nov. 2009.
[27] J. Zhao and G. Cao, "VADD: vehicle-assisted data delivery in vehicular ad hoc networks," *IEEE Trans. Veh. Technol.*, vol. 57, no. 3, pp. 1910-1922, May 2008.
[28] L. Zhang, B. Yu and J. Pan, "GeoMob: A mobility-aware geocast scheme in metropolitans via taxicabs and buses," in *Proc. IEEE INFOCOM*, 2014, Toronto, pp. 1279-1787.
[29] H. Xie, A. Boukerche and A. Loureiro, "A multipath video streaming solution for vehicular networks with link disjoint and node-disjoint," *IEEE Trans. Parall. Distr. Syst.*, vol. pp, no. 99, pp. 1-14, Nov. 2014.
[30] S. Lam and C. Qian, "Geographic routing in d-dimensional spaces with guaranteed delivery and low stretch," *IEEE/ACM Trans. Netw.*, vol. 21, no. 2, pp. 663-677, Apr. 2013.
[31] L. Liu and H. Ma, "On coverage of wireless sensor networks for rolling terrains," *IEEE Trans. Parall. Distr. Syst.*, vol. 23, no.1, pp. 118-125, Jan. 2012.
[32] L. Zhu, C. Li, Y. Wang, Z. Luo, Z. Liu, B. Li and X. Wang, "On Stochastic Analysis of Greedy Routing in Vehicular Networks," *IEEE Trans. Intell. Transp. Syst.*, vol. pp, no. 99, pp. 1-14, Jul. 2015. DOI: 10.1109/TITS.2015.2446771.
[33] S. Ahn, M. Cassidy and J. Laval, "Verification of a simplified car-following theory," *Transportation Research Part B: Methodological*, vol. 38, no. 5, pp. 431-440, Jun. 2004.
[34] L. Cheng and S. Panichpapiboon, "Effects of Intervehicle Spacing Distributions on connectivity of vanet: a case study from measured highway traffic," *IEEE Commun. Mag.*, vol. 50, no. 10, pp. 90-97, Oct. 2012.
[35] Feng Xue and P. R. Kumar, "The number of neighbors needed for connectivity of wireless networks," *Wireless Networks*, vol. 10, no. 2, pp. 169-181, Mar. 2004.
[36] The network simulator ns-2, http://www.isi.edu/nsnam/ns.
[37] Y. Zhu, Y. Qiu, Y. Wu and B. Li, "On adaptive routing in urban vehicular networks," in *Proc. IEEE GLOBECOM*, 2012, Anaheim, pp. 1593-1598.
[38] X. Zhang, K. Chen, X. Cao and D. Sung, "A street-centric routing protocol based on micro topology in vehicular ad hoc networks," *IEEE Trans. Veh. Technol.*, vol. pp, no. 99, pp. 1-15, July 2015.
[39] VanetMobiSim Project, http://vanet.eurecom.fr.

Lina Zhu received her B.E. degree from Suzhou University of Science and Technology, Suzhou, China, in 2009, and is currently pursuing the Ph.D. degree in telecommunication engineering, at Xidian University, Xi'an, China. Her current research interests include mobility model, routing and MAC protocols in vehicular networks.

Changle Li (M'09) received the B.E. degree in Microwave Telecommunication Engineering, M.E. and Ph.D. degrees in Communication and Information System, from Xidian University, China, in 1998, 2001 and 2005, respectively. From 2006 to 2007, he was with Computer Science Department at University of Moncton, Canada as a postdoctoral researcher. From 2007 to 2009, he was an expert researcher at National Institute of Information and Communications Technology (NICT), Japan. He is currently a professor in State Key Laboratory of Integrated Services Networks at Xidian University, China. His research interests include intelligent transportation systems (ITS), vehicular networks, mobile ad hoc networks, and wireless sensor networks.

Bingbing Li received the Ph.D in Communication and Information System from Xidian University, Xi'an, China, in 1995. He is currently a professor in State Key Laboratory of Integrated Services Networks at Xidian University, China. His research interests include digital communication, multirate signal processing, and wireless communication system.

Xinbing Wang (SM'12) received the B.S. degree (with hons.) in automation from Shanghai Jiao Tong University, Shanghai, China, in 1998, the M.S. degree in computer science and technology from Tsinghua University, Beijing, China, in 2001, and the Ph.D. degree with a major in electrical and computer engineering and minor in mathematics from North Carolina State University, Raleigh, in 2006. Currently, he is a professor with the Department of Electronic Engineering, Shanghai Jiao Tong University. His research interests include resource allocation and management in mobile and wireless networks, TCP asymptotics analysis, wireless capacity, cross-layer call admission control, asymptotics analysis of hybrid systems, and congestion control over wireless ad hoc and sensor networks. Dr. Wang has been a member of the Technical Program Committees of several conferences including ACM MobiCom 2012, ACM MobiHoc 2012, IEEE INFOCOM 2009-2013.

Guoqiang Mao (S'98-M'02-SM'08) received PhD in telecommunications engineering in 2002 from Edith Cowan University. He currently holds the position of Professor of Wireless Networking, Director of Center for Real-time Information Networks at the University of Technology, Sydney. He has published more than 100 papers in international conferences and journals, which have been cited more than 3000 times. His research interest includes intelligent transport systems, applied graph theory and its applications in telecommunications, wireless sensor networks, wireless localization techniques and network performance analysis.